Chemistry of Butadienesulfinate Salts with (Cp*RhCl2)2 and the Reactivity of Their Derivatives with Tertiary Phosphines

ARTICLE *in* ORGANOMETALLICS · JULY 2010

Impact Factor: 4.13 · DOI: 10.1021/om901108y

ORGANOMETALLICS
Article

Organometallics **2010,** *29,* 3709–3721 3709
DOI: 10.1021/om901108y

Chemistry of Butadienesulfinate Salts with $(Cp^*RhCl_2)_2$ and the Reactivity of Their Derivatives with Tertiary Phosphines

Brenda A. Paz-Michel, Felipe J. González-Bravo, Lindsay S. Hernández-Muñoz, and M. Angeles Paz-Sandoval*

Departamento de Química, Centro de Investigación y de Estudios Avanzados del IPN Avenida IPN # 2508, San Pedro Zacatenco, C. P. 07360, D. F., México

Received December 22, 2009

The reaction of dinuclear $(Cp^*RhCl_2)_2$ (**1**) with the lithium butadienesulfinate salt Li[$SO_2CH{=}CHCH{=}CH_2$] (**2-Li**) in THF results in the formation of dimeric [$Cp^*Rh(Cl)_2$(5-η-$SO_2CH{=}CRCH{=}CHR$)(Li)(THF)]$_2$ (**3**) in 82% yield, while an excess of potassium butadienesulfinate, K[$SO_2CH{=}CHCH{=}CH_2$] (**2-K**), affords the mononuclear rhodium ion pair [Cp^*RhCl(5-η-$SO_2CH{=}CH{-}CH{=}CH_2$)(5-η-$S(O_2^-K^+)CH{=}CHCH{=}CH_2$)] (**5-K**) in 90% yield. Compound **5-K** reacts with $AgBF_4$ to give the neutral compound [Cp^*Rh(1,2,5-η-$SO_2CH{=}CHCH{=}CH_2$)(5-η-$SO_2CH{=}CHCH{=}CH_2$)] (**6**) in 67% yield. The lability and low stability of **5-K** as well as that of compound **3** were established by NMR and dynamic light scattering. A mixture of **5-K** with 5 equiv of **2-K**, under THF reflux, shows spectroscopic evidence of the trisubstituted [Cp^*Rh(5-η-$SO_2CH{=}CHCH{=}CH_2$)$_2$(5-η-$S(O_2^-K^+)CH{=}CHCH{=}CH_2$)] (**7-K**), which, in the presence of KCl, is in equilibrium with **5-K**, thus preventing its isolation. By ESI-TOF-MS experiments of this mixture, the presence of aggregated species **5-K**(**2-K**)$_n$ and **7-K**(**2-K**)$_n$ (n = 1−3) has been detected. Organometallic−butadienesulfinate aggregates contrast with ruthenium complexes previously observed with butadienesulfonyl and butadienesulfinate ligands. Reactions of **3** and **5-K** toward PR_3 (R = Ph, Me) are not selective and afford mixtures of compounds [Cp^*RhCl(5-η-$SO_2CH{=}CHCH{=}CH_2$)(PR_3)] [R = Ph, (**8**); Me, (**10**)] and $Cp^*Rh(Cl)_2PR_3$ [R = Ph, (**9**) Me, (**11**)]. The butadienesulfonyl ligands in **8** and **10** are in *S*- or *W*-conformation for the corresponding kinetic and thermodynamic products. Compound **3** favors the formation of **9** or **11**, while **5-K** favors that of isomer **8** or **10**.

Introduction

The butadiensulfonyl complexes Cp^*MCl(5-η-$SO_2CH{=}CHCH{=}CH_2$)PR_3 (M = Rh, Ir; R = Ph, Me) have recently been prepared by reaction of $Cp^*MCl_2PR_3$ with K[$SO_2CH{=}CHCH{=}CH_2$).[1] Prior to these reports, the only examples of butadienesulfonyl derivatives were compounds [$Cp^*Ir(Cl)_2$(5-η-$SO_2CH{=}CRCH{=}CHR$)(Li)(THF)]$_2$ and [Cp^*IrCl(1,2,5-η-$SO_2CH{=}CRCH{=}CH_2$)] (R = H, Me) obtained from $(Cp^*IrCl_2)_2$ and the corresponding lithium and potassium butadienesulfinate salts, respectively.[2] The develop of an efficient and easy synthetic procedure, along with the rich and versatile chemistry of the butadienesulfinate salts depending on the alkaline metal[3] and transition metal involved[1,2,4] have gained our attention, since they could be interesting ligands in material science, once they could establish intermolecular interactions and could act as amphoteric ligands. A comparative study between the reactivity of the "Cp^*MCl" moiety with the butadienesulfinate salts Li($SO_2CH{=}CRCH{=}CHR$) (R = H, Me) (**2-Li**) or K($SO_2CH{=}CRCH{=}CHR$) (R = H, Me) (**2-K**) has been carried out, specifically for $(Cp^*RuCl)_4$[4] and $(Cp^*IrCl_2)_2$,[2] which has shown interesting analogies or significant differences. The crystalline structures of dinuclear compounds [$Cp^*Ir(Cl)_2$(5-η-$SO_2CH{=}CRCH{=}CHR$)(Li)(THF)]$_2$[2] reveal the presence of metallacyclic, five- and eight-membered rings, which break easily to afford mononuclear compounds Cp^*IrCl(1,2,5-η-$SO_2CH{=}CRCH{=}CHR$) (R = H, Me), upon displacement of THF and LiCl. Contrastingly, immediate formation of compound Cp^*IrCl(1,2,5-η-$SO_2CH{=}CHCH{=}CH_2$) can be achieved if potassium butadienesulfinate salt is used, which shows that the alkaline metal is crucial in the isolation of dinuclear or mononuclear compounds (Scheme 1).

The reaction of the tetranuclear $(Cp^*RuCl)_4$ with the corresponding lithium butadienesulfinate salts Li[$SO_2CH{=}CR'CH{=}CHR$] (R = R′ = H ; R = H, R′ = Me; R = R′ = Me) in THF results in the formation of the corresponding tetrameric [Cp^*Ru(1,2,5-η-$SO_2CH{=}CR'CH{=}CHR$)$LiCl]_4$ complexes, whereas if potassium salts are used, mononuclear allylsulfene ruthenium compounds [Cp^*Ru(1−5-η-$SO_2CH{=}CR'CH{=}CHR$)] (R = R′ = H; R = H, R′ = Me) are isolated[4] (Scheme 1).

*To whom correspondence should be addressed. E-mail: mpaz@cinvestav.mx.

(1) Paz-Michel, B. A.; Cervantes-Vasquez, M.; Paz-Sandoval, M. A. *Inorg. Chim. Acta* **2008**, *361*, 3094.
(2) Gamero-Melo, P.; Cervantes-Vasquez, M.; Sanchez-Castro, M. E.; Ramirez-Monroy, A.; Paz-Sandoval, M. A. *Organometallics* **2004**, *23*, 3290.
(3) Gamero-Melo, P.; Villanueva-Garcia, M.; Robles, J.; Contreras, R.; Paz-Sandoval, M. A. *J. Organomet. Chem.* **2005**, *690*, 1379.
(4) Paz-Michel, B. A.; Gonzalez-Bravo, F. J.; Hernandez-Muñoz, L. S.; Paz-Sandoval, M. A. *Organometallics*, **2010**, DOI: 10.1021/om901107n.

Published on Web 07/30/2010

Scheme 1

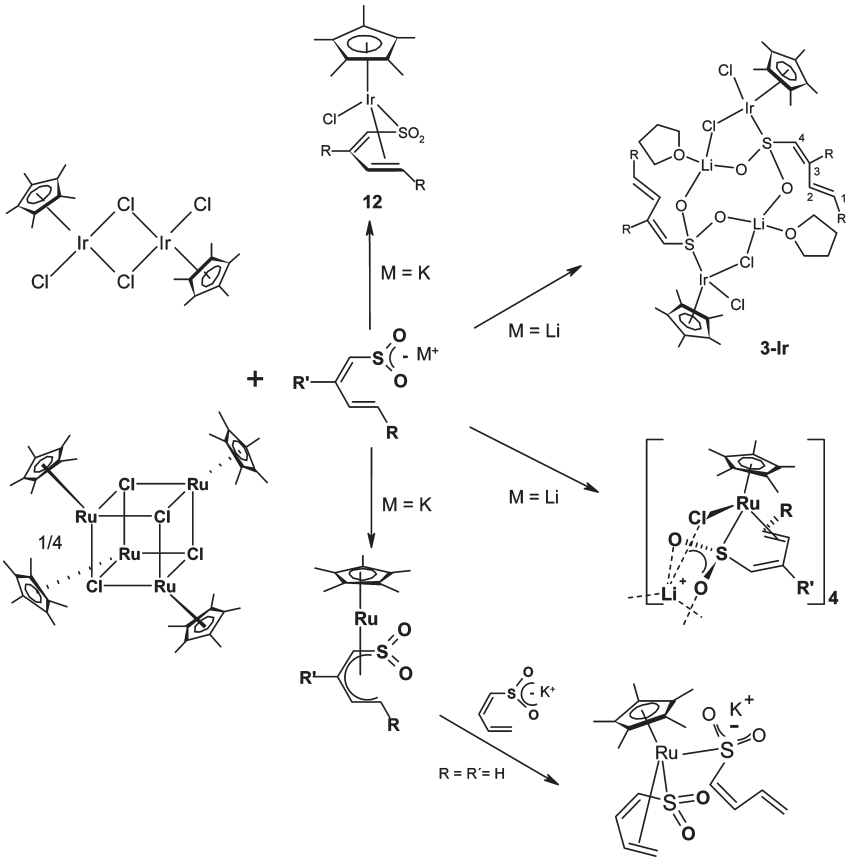

Interestingly, tetrameric and monomeric ruthenium compounds easily interconvert in the presence of H_2O or LiCl, respectively. A comparative study of the dissociation of tetramers $(Cp^*RuCl)_4$ and $[Cp^*Ru(1,2,5\text{-}\eta\text{-}SO_2CH{=}CH\text{-}CH{=}CH_2)LiCl]_4$, in THF, via dynamic light scattering (DLS) measurements shows a clear tendency for $(Cp^*RuCl)_4$ to form polydisperse aggregates, while the butadienesulfonyl tetranuclear structure remains significantly preserved.[4] Novel ion-pair complexes $[Cp^*Ru(1,2,5\text{-}\eta\text{-}SO_2CH{=}CHCH{=}CH_2)(5\text{-}\eta\text{-}S(O_2^-M^+)CH{=}CHCH{=}CH_2)]$ (M = K, Ag, *n*-Bu_4N) have been characterized by ^1H and $^{13}C\{^1H\}$ NMR, IR, ESI-TOF-MS, and cyclic voltammetry. Species such as $[Cp^*Ru(5\text{-}\eta\text{-}SO_2CH{=}CHCH{=}CH_2)(5\text{-}\eta\text{-}S(O_2^-M^+)CH{=}CHCH{=}CH_2)_2]$ (M = Li, K) and $[Cp^*Ru(1,2,5\text{-}\eta\text{-}SO_2CH{=}CHCH{=}CH_2)(5\text{-}\eta\text{-}S(O_2^-M^+)CH{=}CHCH{=}CH_2)]_n$ (n = 2, 3, M = Li and/or K) have been detected by spectrometric studies and have given evidence of the tendency of the SO_2 fragment to afford oligomers according to the cations employed.[4] Herein, this study extends the corresponding comparative studies to reactions of rhodium dimer $(Cp^*RhCl_2)_2$ with butadienesulfinate salts $Li[SO_2CH{=}CHCH{=}CH_2]$ (**2-Li**) and $K[SO_2CH{=}CHCH{=}CH_2]$ (**2-K**), which respectively afford compounds $[Cp^*Rh(Cl)_2(5\text{-}\eta\text{-}SO_2CH{=}CHCH{=}CH_2)(Li)(THF)]_2$ (**3**) and $[Cp^*RhCl(5\text{-}\eta\text{-}SO_2CH{=}CHCH{=}CH_2)(5\text{-}\eta\text{-}S(O_2^-K^+)CH{=}CHCH{=}CH_2)]$ (**5-K**). The addition reaction of **3** and **5-K** with PMe_3 and PPh_3 is discussed, and the metathesis reaction between $[Cp^*Rh(Cl)_2(PR_3)]$ (M = Ph, Me) and **2-K**, previously reported, is comparatively described. The metathesis reaction is more selective and affords mononuclear *S*- and *W*-isomers $[Cp^*RhCl(5\text{-}\eta\text{-}SO_2CH{=}CHCH{=}CH_2)(PR_3)]$ (R = Ph, Me).[1]

Results and Discussion

Reactivity of $(Cp^*RhCl_2)_2$ (1) with 2-M (M = Li, K). As shown in Scheme 2, treatment of $(Cp^*RhCl_2)_2$ (**1**) with the lithium butadienesulfinate **2-Li**[3] leads to the formation of $[Cp^*Rh(Cl)_2(5\text{-}\eta\text{-}SO_2CH{=}CHCH{=}CH_2)(Li)(THF)]_2$ (**3**), in 82% yield,[1,5] which is isoelectronic to **3-Ir** as observed in the iridium chemistry (Scheme 1). Compound **3** was more labile and less stable than the corresponding iridium complex **3-Ir**.[2]

The η^1-bonding mode of the butadiensulfonyl ligand in **3** was evident from the ^1H and $^{13}C\{^1H\}$ NMR spectra, in which an *S*-conformation was observed (5.20, $H1_{gem}$; 5.39, $H1'_{gem}$; 8.19, H2; 5.98, H3; 6.79, H4; $J_{1,2}$ = 17.0 Hz, $J_{1',2}$ = 8.9 Hz, $J_{2,3}$ = 11.2, $J_{3,4}$ = 11.0). The highest frequency signal, assigned to H2, suggested an interaction between H2 and one of the oxygen atoms from the SO_2 moiety, which was also supported in the solid state of **3** [H2−O2, 2.37(6) Å] and $[Cp^*RhCl(5\text{-}\eta\text{-}SO_2CH{=}CHCH{=}CH_2)PMe_3]$ (**10-*S***) [H2−O1, 2.366(8) Å] (*vide infra*), as well as in **3-Ir** [H2−O2, 2.451(40) Å] and $[Cp^*IrCl(5\text{-}\eta\text{-}SO_2CH{=}CHCH{=}CH_2)PR_3]$ [H2−O1, R = Ph (**8-*S*-Ir**) (2.414(7) Å); Me (**10-*S*-Ir**) H2−O1 (2.3782(83) Å)] (*vide infra*).[1] The ^{13}C NMR of **3** for C1, C2, C3, and C4 at 123.8, 133.0, 132.7, and 136.5 confirmed that the butadiene fragment was not coordinated.

The crystal structure of **3** is depicted in Figure 1, and crystal data as well as bond lengths and angles are given in Tables 1 and 2, respectively. The solid-state structure is analogous to iridium **3-Ir**[2] (Scheme 1), where there are two metallacyclic five-membered rings (Li1−O1−S−Rh−Cl2)

(5) Paz-Sandoval, M. A.; Rangel-Salas, I. I. *Coord. Chem. Rev.* **2006**, *250*, 1071.

Scheme 2

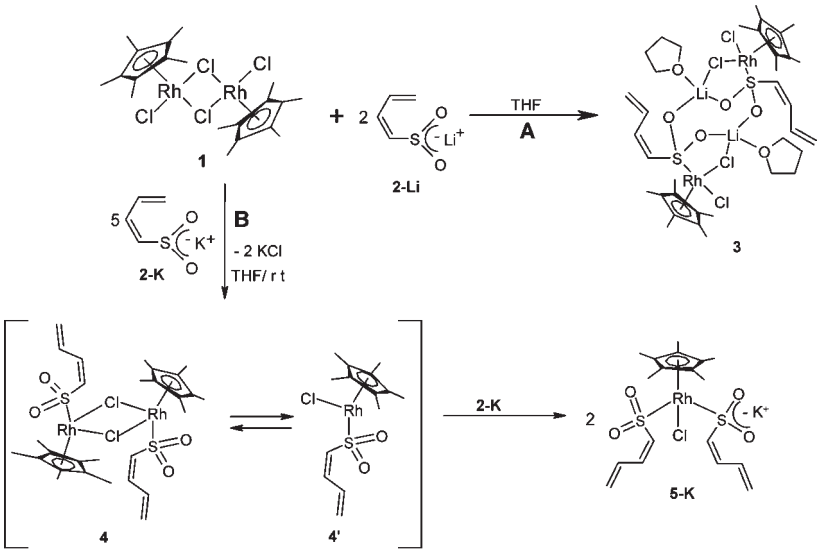

and one eight-membered ring (Li1−O1−S2−O2−Li1−O1−S2−O2).

Four hydrogen bonds are also formed, hence inducing pseudo-rings of six and five members among H2−O2−S2−C4−C3−C2 and H4−Cl1−Rh1−S2−C4, respectively, where the distances of H2−O2 and H4−Cl1 are 2.37(6) and 2.89(4) Å. The conformation of the butadienesulfinate ligand is *S*-shaped [torsion angle C1−C2−C3−C4; −178.0-(0.51)°] and the diene (C1−C2 [1.325(6) Å] and C3−C4 [1.337(5) Å]) is not coordinated to the rhodium as observed in solution (*vide supra*). These C=C bond lengths are longer than those of **3-Ir** [C1−C2, 1.318(13) and C3−C4, 1.333(11) Å],[2] and Rh−S [2.3060(8) Å] is longer than Ir−S [2.2965(17) Å].[2] The rhodium atom is also coordinated to Cp* and two chloro atoms [2.4064(9) and 2.4156(8) Å], in which the longer Rh−Cl bond length corresponds to the chloro interacting with the Li atom, which acts as a bridge between both units through the eight-membered ring. Each Li atom interacts with Cl2 [2.396(6) Å] and O1 [1.899(6) Å] from one of the fragments [Cp*Rh(Cl)$_2$(5-η-SO$_2$CH=CHCH=CH$_2$)] and with the O2 atom of the SO$_2$ fragment from the complementary unit. The sphere of coordination is completed once the THF adduct [O3−Li, 1.954(6) Å] is formed. The bond lengths Li1−Cl2 and Li1−O3 are approximately 0.32 and 0.18 Å shorter than those of **3-Ir**. Both distances S2−O1 [1.479(2) Å] and S2−O2 [1.480(2) Å] are quite similar, which implies formal double bonds.

In the iridium chemistry, the reaction of **2-K** with [Cp*IrCl$_2$]$_2$ affords compound Cp*IrCl(1,2,5-η-SO$_2$CH=CHCH=CH$_2$) (**12**) in 83% yield,[2] (Scheme 1), and it can also be immediately isolated if **3-Ir** is in CDCl$_3$, due to elimination of LiCl and THF. Contrastingly, the mononuclear rhodium analogue, under similar conditions, was not even detected.

Compound **3** was quite unstable in CDCl$_3$ solution and required low temperature for its preservation. Nevertheless, after 3 h, it decomposed with evidence of regeneration of dimer [Cp*RhCl$_2$]$_2$ (**1**). The reaction of an equimolar mixture of **1** with **2-K** in THF, at low temperature or even after 10 h at room temperature, always showed a significant amount of **1**. A higher excess of **2-K** was always required in order to consume **1**. When a mixture of **1** and 5 equiv of **2-K** was

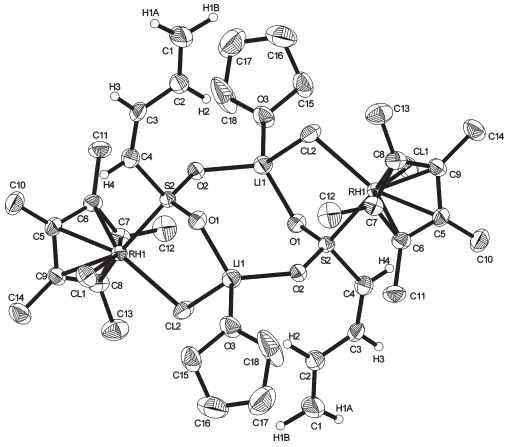

Figure 1. Crystal structure of compound [Cp*Rh(Cl)$_2$(5-η-SO$_2$CH=CHCH=CH$_2$)(Li)(THF)]$_2$ (**3**).

stirred in THF for 2 h at room temperature, an orange solid of [Cp*RhCl(5-η-SO$_2$CH=CHCH=CH$_2$)(5-η-S(O$_2^-$K$^+$)-CH=CHCH=CH$_2$)] (**5-K**) was isolated in 90% yield (Scheme 2). The rhodium atom is coordinated to a Cp*, a chloro atom, and the butadienesulfonyl and butadienesulfinate ligands; the last two are exclusively bound through the sulfur atom. The *S*-conformation was confirmed in both sulfur ligands. Cyclic voltammetry confirmed the presence of an ion-pair complex in **5-K**, therefore discriminating the formation of an anionic organometallic compound (*vide infra*). Previous studies with (Cp*RuCl)$_4$ and **2-K** have shown the formation of a similar compound, [Cp*Ru(1,2,5-η-SO$_2$CH=CHCH=CH$_2$)(5-η-S(O$_2^-$K$^+$)CH=CHCH=CH$_2$)] (Scheme 1), where the butadiensulfonyl coordinates $\eta^{2,1}$ through the terminal double bond and the sulfur atom, whereas the potassium butadienesulfinate salt coordinates exclusively through the free electron pair of the sulfur atom. The ruthenium ion-pair complex can exchange the cation selectively in order to give other novel ion pairs such as [Cp*Ru(1,2,5-η-SO$_2$CH=CHCH=CH$_2$)(5-η-S(O$_2^-$M$^+$)-CH=CHCH=CH$_2$)] (M = Ag, *n*-Bu$_4$N), while **5-K** with AgBF$_4$ affords [Cp*Rh(1,2,5-η-SO$_2$CH=CHCH=CH$_2$)(5-η-SO$_2$CH=CHCH=CH$_2$)] (**6**) by elimination of AgCl and

Table 1. Crystal Data and Experimental Parameters for Compounds 3, 9, and 10-*S*

	3	**9**	**10-*S***
formula	$C_{36}H_{56}Cl_4Li_2O_6Rh_2S_2$	$C_{22}H_{25}Cl_2PRh$	$C_{17}H_{29}ClO_2PRhS$
fw	1010.43	690.67	466.79
cryst syst	monoclinic	monoclinic	orthorrombic
space group	$P2_1/n$	$P2_1/n$	$P2_12_12_1$
a (Å)	8.2770(2)	8.6838(2)	9.0420(5)
b (Å)	14.5844(3)	16.2280(4)	12.5070(6)
c (Å)	18.0031(5)	21.3511(6)	18.1640(13)
β (deg)	90.4550(10)	97.8230(10)	90
V (Å^3)	2173.18(9)	2980.81(13)	2054.1(2)
Z	2	4	4
D_{calc} (g/cm^3)	1.544	1.539	1.509
size (mm)	0.65 × 0.55 × 0.35	0.33 × 0.13 × 0.05	0.25 × 0.03 × 0.02
range h,k,l	$-10 \le h \le 10$	$-10 \le h \le 11$	$-11 \le h \le 7$
	$-18 \le k \le 18$	$-20 \le k \le 21$	$-16 \le k \le 16$
	$-23 \le l \le 23$	$-27 \le l \le 27$	$-13 \le l \le 23$
2θ range (deg)	7.28 to 54.98	5.34 to 54.94	6.00 to 55.00
no. of reflns collected	17 542	27 179	9753
no. of unique reflns	4894 (R_{int} = 0.0393)	6796 (R_{int} = 0.0887)	4499 (R_{int} = 0.0807)
abs corr (T_{max}, T_{min})	1.0, 0.9468	0.9474, 0.7144	0.9774, 0.7625
R_w	0.0379	0.0697	0.0649
wR_2 (all data)	0.1044	0.1765	0.0943
gof	1.116	1.052	0.958

Table 2. Selected Bond Lengths and Angle of Compounds 3 and 10-*S*

	bond lengths (Å)				bond angles (deg)		
	3		**10-*S***		**3**		**10-*S***
C1−C2	1.325(6)		1.316(13)	Cl1−Rh1−S2	89.21(3)	Cl1−Rh1−S1	91.70 (9)
C2−C3	1.440(5)		1.425(14)	C4−S2−Rh1	107.52(13)	C4−S1−Rh1	104.0 (3)
C3−C4	1.337(5)		1.395(14)	C4−S2−O2	106.60(15)	C4−S1−O2	100.7 (5)
C4−S2	1.782(3)		1.834(11)	C4−S2−O1	103.94(16)	C4−S1−O1	107.1 (5)
S2−O1	1.479(2)	S1−O1	1.398(7)	C4−C3−C2	128.7(3)		123.5 (11)
S2−O2	1.480(2)	S1−O2	1.464(7)	O1−S2−O2	112.35(14)	O1−S1−O2	115.8 (4)
Rh1−Cl1	2.4064(9)		2.396(2)	C1−C2−C3	121.8(4)		119.1 (13)
Rh1−S2	2.3060(8)	Rh1−S1	2.308(2)	O1−S2−Rh1	114.26(10)	O1−S1−Rh1	110.3 (3)
Rh1−Cl2	2.4156(8)			O2−S2−Rh1	111.48(10)	O2−S1−Rh1	117.1 (3)
Cl2−Li1	2.396(6)	Rh1−P1	2.283(3)	Cl2−Rh1−S2	87.26(3)		
Li1−O1	1.899(6)			Cl2−Rh1−Cl1	92.43(3)	P1−Rh1−S1	89.67 (9)
Li1A−O2	1. 920(6)			O1−Li1−Cl2	96.1(3)	Cl1−Rh1−P1	88.28 (9)
Li1−O3	1.954(6)			C3−C4−S2	127.9(3)	C3−C4−S1	128.4 (9)
O2−H2	2.37(6)	O2−H1	2.367(7)				
Cl1−H4	2.89(4)	Cl1−H4	2.911(3)				
Li1−S2	2.986(6)						

KBF_4 (*vide infra*). In the iridium chemistry, there is also evidence of formation of the ion-pair complex [Cp*IrCl(5-η-$SO_2CH{=}CHCH{=}CH_2$)(5-η-$S(O_2^-K^+)CH{=}CHCH{=}CH_2$)] (**5-K-Ir**), but always in a mixture with [Cp*Ir(1,2,5-η-$SO_2CH{=}CHCH{=}CH_2$)(5-η-$SO_2CH{=}CHCH{=}CH_2$)] (**6-Ir**) and compound [Cp*IrCl(1,2,5-η-$SO_2CH{=}CHCH{=}CH_2$)] (**12**), the former being in smaller amount.[6a] The ^{1}H and $^{13}C\{^1H\}$ NMR spectra of **5-K** showed only one pattern of signals for both butadienesulfonyl and butadienesulfinate ligands, as described in the Experimental Section, even though they behaved as neutral and ion-pair ligands (see Supporting Information). The chemical shifts and coupling constants of the sulfone ligands in **3** and **5-K** confirmed a similar bonding mode and an *S*-conformation. The IR spectra of the S=O region of **5-K** with an ion pair (delocalized S···O bond) and a neutral ligand (formal double bond, S=O) did not show significant differences in the corresponding band shapes, in contrast to what happens with ruthenium derivatives, which could be distinguished between butadienesulfonyl or butadienesulfinate coordinated ligands.[4] The stability of **5-K** in solution was moderate, it decomposed after 24 h in $CDCl_3$ or 1 h under refluxing acetone, but compared with **3**, it was more robust.

The formation of **5-K** results from combined reactions, as described in the mechanism proposed in Scheme 3.

First, the metathesis reaction of **1** and **2-K** affords KCl and the equilibrium mixture of **4** and **4′** (i). Subsequent addition

(6) Cervantes-Vasquez, M.; Paz-Sandoval, M. A. Unpublished results: (a) Compounds $(Cp^*IrCl_2)_2$ (269.0 mg, 0.338 mmol) and 5 equiv of $K[SO_2CH{=}CHCH{=}CH_2]$ (264.0 mg, 1.69 mmol) were dissolved in THF (20 mL). After 2.5 h of stirring at room temperature, the mixture was filtered and the solvent reduced under vacuum. Addition of pentane afforded a yellow solid, which after filtration showed through the ^{1}H NMR to be a mixture of **5-K-Ir**, **6-Ir**, and **12** in 1.7:6.3:2.0 ratio, respectively. If a higher excess (10 equiv) of **2-K** is used, the mixture of products is in a 2.1:4.9:3.0 ratio. (b) Compound $(Cp^*IrCl_2)_2$ (100.0 mg, 0.125 mmol) was dissolved in THF (10 mL) to form an orange solution, which was cooled at −110 °C (liq N_2/EtOH). A suspension of Li-$[SO_2CH{=}CHCH{=}CH_2]$ (31.0 mg, 0.250 mmol) in THF (8 mL) was added, and it was allowed to reach room temperature. Immediately after the addition, the solution became a light yellow-orange suspension, and after 2 h of stirring at room temperature, a yellow-orange solution was observed. The solution was filtered and PPh_3 (66.0 mg, 0.250 mmol) was added. The reaction mixture was stirred 1.5 h, filtered, and evaporated until dryness. The ^{1}H and ^{31}P NMR showed a nonseparable mixture of **8-*S*-Ir** and **9-Ir**. (c) As described above in (b), but adding PMe_3 (27.0 μL, 0.250 mmol) at −110 °C. The spectroscopic evidence showed formation of compounds **10-*S*-Ir**, **11**, and **12**. (d) Reaction of compound **12** and PPh_3 gave a mixture of compounds **8-*S*-Ir**, **9**, and **12**, from which **8-*S*-Ir** affords single crystals, after crystallization by indirect diffusion of $CDCl_3$/hexane at room temperature.

Scheme 3

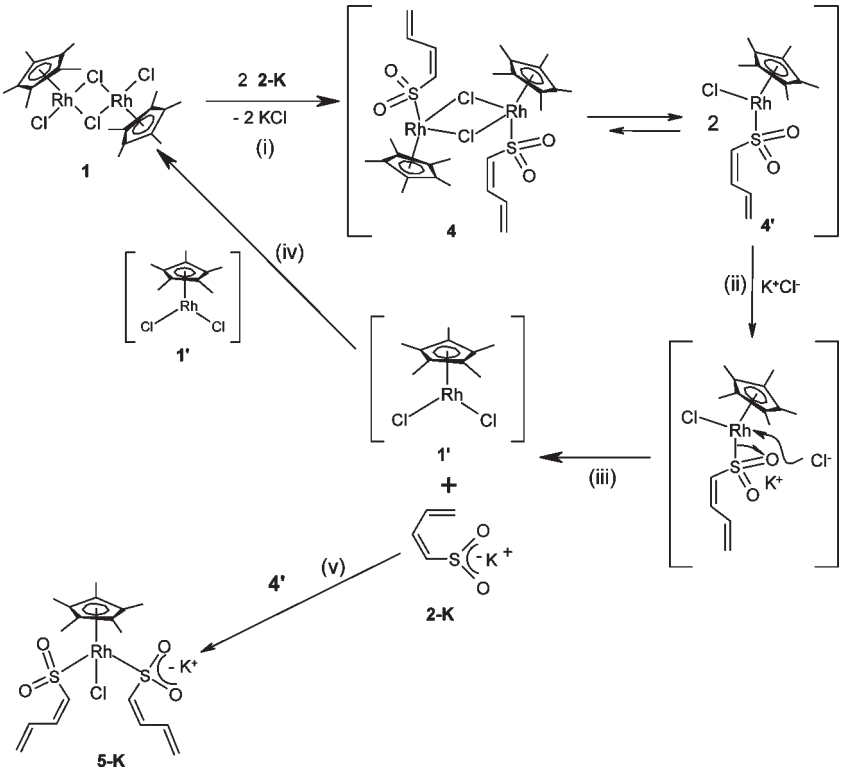

of KCl to **4′** (ii) induces the migration of one electron from the Rh−S bond to the sulfone fragment. The neutralization of the negative charge with the potassium cation leads to the regeneration of **2-K** and the consequent formation of **1′** (iii). Finally, two molecules of **1′** afford compound **1** (iv), while addition of **2-K** to **4′** gives **5-K** (v).

The formation of species **4** is supported by the existence of the well-known dimeric compound **1** and by different kinds of dinuclear chloro-bridged compounds,[7−13] which are obtained from metathesis or addition reactions on **1**. The ^{1}H NMR spectrum of an equimolar reaction of **1** with **2-K**, in THF and after 2−10 h at room temperature, showed the presence of **1** along with a highly reactive species, for which there is no coordination of the butadiene fragment of the sulfonyl ligand. The prevalence of **1** can be explained by reaction of KCl with **4′** and consequent elimination of **2-K**. This fact was confirmed when the consumption of **1** was achieved when a higher excess of **2-K** was added to the reaction mixture.

In order to confirm the presence of the ion pair in **5-K**, cyclic voltammetry was carried out. In agreement with previous voltammetric studies on the ion pair [Cp*Ru(1,2,5-η-SO_2-CH=CHCH=CH_2)(5-η-S($O_2^-K^+$)CH=CHCH=CH_2)],[4,14] the establishment of a dissociation equilibrium was expected in which the nonassociated negative charge showed lower oxidation potential values than those for the corresponding associated ion pair. That is actually what we observed in **5-K**, promoted by the novel interaction of the potassium butadienesulfinate ligand **2K**.

The electrochemical oxidation of compound **5-K** with n-Bu_4NBF_4 as supporting electrolyte in THF showed several peaks, as described in Figure 2. The less positive signal IA is assigned to the oxidation of the negative charge of the nonassociated sulfone anion $\mathbf{5}^-$, which is formed by cation exchange, after the addition of **5-K** to the n-Bu_4NBF_4 solution (eq 1). This statement is based on the similar voltammetric behavior observed in the ruthenium ion pair [Cp*Ru(1,2,5-η-SO_2CH=CHCH=CH_2)(5-η-S($O_2^-K^+$)CH=CHCH=CH_2)].[4] However, in rhodium chemistry, the presence of chloro in **5-K** led to a collateral reaction that involved the chloro elimination and formation of the neutral compound [Cp*Rh(1,2,5-η-SO_2CH=CHCH=CH_2)-(5-η-SO_2CH=CHCH=CH_2)] (**6**) (described as Rh-SO_2 in eq 1).

$$\underset{\mathbf{5\text{-}K}}{\text{Rh-SO}_2^-\,K^+} + n\text{-Bu}_4N^+BF_4^- \rightleftarrows \underset{\mathbf{5}^-}{\text{Rh-SO}_2^-} + n\text{-Bu}_4N^+ + K^+BF_4^-$$

$$\underset{\mathbf{5}^-}{\text{Rh-SO}_2^-} \rightleftarrows \underset{\mathbf{6}}{\text{Rh-SO}_2} + Cl^- \qquad (1)$$

Peak IIIA was assigned to the oxidation of the rhodium atom either in **5-K** or in the dissociated species $\mathbf{5}^-$ (Figure 2A).

(7) Yamamoto, Y.; Miyauchi, F. *Inorg. Chim. Acta* **2002**, *334*, 77.
(8) Berenguer, J. R.; Bernechea, M.; Fornies, J.; Gomez, J.; Lalinde, E. *Organometallics* **2002**, *21*, 2314.
(9) Yamamotoa, Y.; Suzuki, H.; Tajima, N.; Tatsumi, K. *Chem.—Eur. J.* **2002**, *8*, 372.
(10) Gauthier, S.; Quebatte, L.; Scopelliti, R.; Severin, K. *Chem.—Eur. J.* **2004**, *11*, 2811.
(11) Gauthier, S.; Scopelliti, R.; Severin, K. *Helv. Chim. Acta* **2005**, *88*, 435.
(12) Ara, I.; Berenguer, J. R.; Eguizabal, E.; Fornies, J.; Lalinde, E.; Martin, A. *Eur. J. Inorg. Chem.* **2001**, 1631.
(13) Valderrama, M.; Contreras, R.; Boys, D. *J. Organomet. Chem.* **2003**, *665*, 7.
(14) Gonzalez Bravo F. J., unpublished results. In the case of tetrabutylammonium carboxylates in acetonitrile, it has been observed in our research group that the oxidation wave is enlarged and shifted toward more positive values when alkaline metal salts are added to the solution, which suggests that the negative charge on the carboxylic function is ion-pairing stabilized, and consequently this is less available for electron transfer. This ion-pairing phenomenon falls in line with the low solubility of the alkaline metal salts of carboxylic acids in polar solvents.

Prewave IIA was attributed to the presence of the chloride ion in the equilibrium mixture, according to a similar potential observed for the oxidation of chloride ion dissociated from *n*-Bu_4NCl in THF (*vide infra*). After 50 min, the voltammetric behavior showed different results (curve B): peak IA disappeared, an increase in the current intensity of the prewave IIA was observed, peak IIIA remained without significant change, and the new peak IVA (1.75 V/SCE) appeared (Figure 2B). The absence of peak IA suggests that species $\mathbf{5}^-$ is no longer present in the equilibrium described in eq 1. The appearance of peak IVA is attributed to the rhodium oxidation in compound **6** by elimination of chloride in $\mathbf{5}^-$, which is in agreement with the increase of the current intensity of prewave IIA. Considering the equilibrium reactions in Scheme 4, it is proposed that formation of **6** is promoted by the exchange of K^+ for *n*-Bu_4N^+, which induces precipitation of KBF_4 and formation of the dissociated ion pair $\mathbf{5}^-$ (i). Compared to **5-K**, the negative charge of the SO_2^- fragment in $\mathbf{5}^-$ can easily be transferred to the rhodium atom and lead to the formation of a covalent Rh−S bond, along with the elimination of chloride and the formation of *n*-Bu_4NCl (ii). Finally, the coordination of the terminal C=C from one of the butadienesulfonyl ligands to the metallic center affords compound **6** (iii) (*vide infra*).

In order to demonstrate that peak IVA corresponds to the oxidation of the rhodium atom in compound **6** and that the prewave IIA is associated with the oxidation of the chloride ion, two independent experiments were carried out in THF and using *n*-Bu_4NBF_4 as supporting electrolyte: **6** (Figure 3B) and *n*-Bu_4NCl (Figure 3C).

The cyclic voltammetry of **6** showed only one peak (Figure 3B), with a potential value corresponding to peak IVA shown in Figures 2B and 3A. According to Figure 3C the oxidation pattern of the chloride ion confirmed that the prewave IIA shown in Figure 2 corresponded to this process. Finally, cyclic voltammetry experiments with compound **6**, in THF and *n*-Bu_4NBF_4 as electrolyte, before and after the addition of *n*-Bu_4NCl, are described in Figure 4.

In the first experiment, the voltammogram showed the expected peak IVA (Figure 4A). After the addition of *n*-Bu_4NCl, a wide peak IIIA appeared (Figure 4B); its position in the potential scale is between the corresponding values for the oxidation of chloride ion and the rhodium atom in **5-K** or $\mathbf{5}^-$ (Figures 2, 3A, and 3C). The broadness of this peak may be understood as overlapped peaks from these oxidation processes.

Two main conclusions are obtained from the electrochemical study: (1) Compound **5-K** has a potassium butadienesulfinate ligand, which acts as a Lewis base through the sulfur atom. (2) In the presence of *n*-Bu_4NBF_4, the ion-pair complex **5-K** participates in two equilibrium reactions: a cationic exchange and an electronic rearrangement that

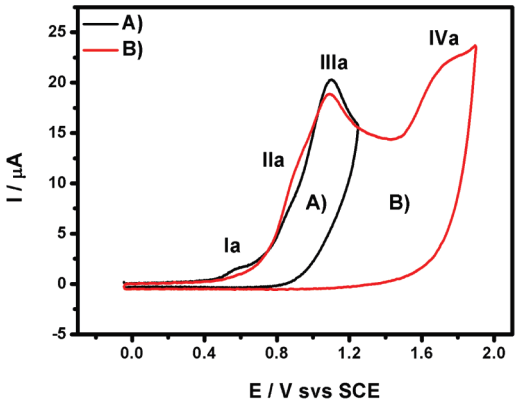

Figure 2. Cyclic voltamperommetry of a solution of **5-K** (2 mM) in THF on a glassy carbon electrode (Φ = 3 mm) at 0.1 V s^{-1}. The supporting electrolyte was *n*-Bu_4NBF_4 0.1 M: (A) t = 0; (B) $t \geq 50$ min.

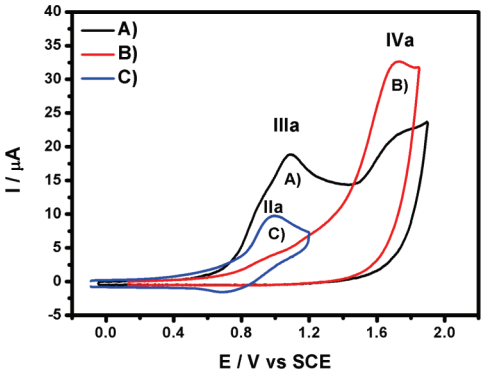

Figure 3. Cyclic voltammetry in THF + 0.1 M *n*-Bu_4NBF_4 on a glassy carbon electrode (Φ = 3 mm) at 0.1 V s^{-1}: (A) **5-K**, 2 mM at $t \geq 50$ min; (B) **6**, 2 mM; and (C) *n*-Bu_4NCl, 2 mM.

Scheme 4

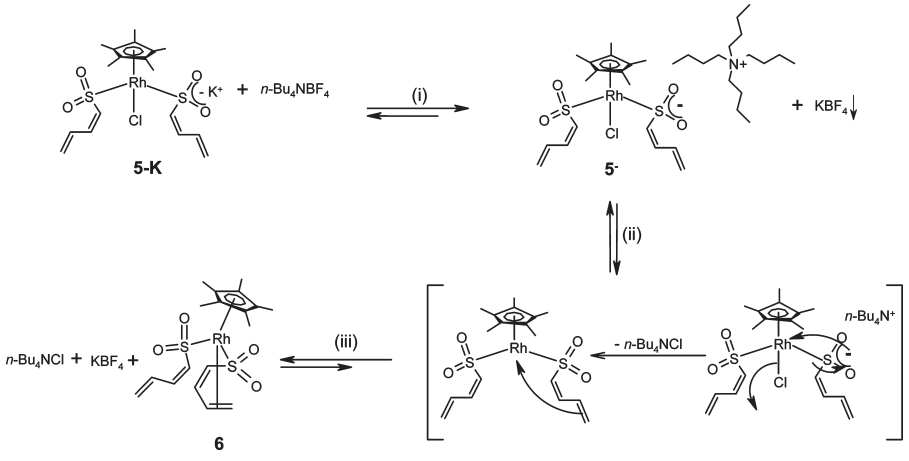

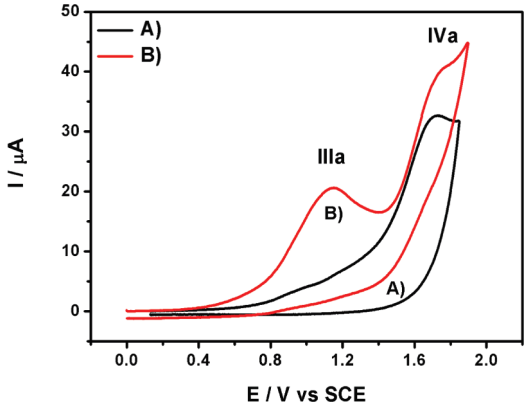

Figure 4. Cyclic voltammetry of a solution of n-Bu_4NBF_4 (0.1M) in THF on a glassy carbon electrode (Φ = 3 mm) at 0.1 V s^{-1}: (A) **6**, 2 mM and (B) **6** after addition of n-Bu_4NCl, 5 mM.

induces the formation of compound **6** along with precipitation of KBF_4 and n-Bu_4NCl.

Compound **6** can be obtained, as a yellow powder in 67% yield, from an equimolar reaction of **5-K** with $AgBF_4$ in THF. ^1H and $^{13}C\{^1H\}$ NMR data are consistent with two butadienesulfonyl ligands that adopt different bonding modes: One is coordinated to the rhodium through the sulfur and the terminal double bond (1,2,5-η-), and the second is coordinated exclusively through the sulfur atom (5-η-) (see Supporting Information).

The lability and low stability of compounds **3** and **5-K**, which were mentioned previously, were confirmed by DLS experiments. For **5-K** two experiments were run: a fresh sample (Figure 5A) and one 1 h later (Figure 5B). For compound **3**, only the acquisition of the fresh sample was analyzed (Figure 5C). The fresh sample of **5-K** behaved as ruthenium compounds [Cp*Ru(1−5-η-$SO_2CH{=}CHCH{=}CH_2$)] and [Cp*Ru(1,2,5-η-$SO_2CH{=}CHCH{=}CH_2$)LiCl]$_4$,[4] thus giving a monodisperse mixture. The analysis of the same sample 1 h later showed the formation of polydisperse species; such a result is in agreement with the complex mixture observed through NMR and mass spectrometry when **5-K** remains in $CDCl_3$ or acetone, respectively. The lability of **5-K** in THF solution resembles the behavior of the tetranuclear ruthenium compound $(Cp^*RuCl)_4$ in the same solvent.[4] Compound **3** showed immediate formation of a polydisperse solution with aggregates of a wide average of diameters (Figure 5C). This result strongly confirms the high lability and instability of complex **3** in THF solution at room temperature and in the presence of air.

The ESI-TOF-MS spectra of the reaction between **1** and excess **2-Li** or **2-K** showed the chloro complexes **5-M** (M = Li, K) as major products, along with evidence of molecular weights that could correspond to dinuclear aggregates $(\mathbf{5\text{-}M})_2$ (M = Li, K). There was no evidence of lithium species with three butadienesulfone ligands, such as compound [Cp*Ru(5-η-$SO_2CH{=}CHCH{=}CH_2$)(5-η-$S(O_2{}^-Li^+)CH{=}CHCH{=}CH_2$)$_2$],[4] which was detected in the ruthenium chemistry. However, it was possible to observe the corresponding trisubstituted-rhodium complex [Cp*Rh(5-η-$SO_2CH{=}CHCH{=}CH_2$)$_2$(5-η-$S(O_2{}^-K^+)CH{=}CHCH{=}CH_2$)] (**7-K**), along with **5-K** and traces of $(\mathbf{5\text{-}K})_2$, when **2-K** was used as a precursor (see Supporting Information). According to these results, a reaction of **5-K** with 5 equiv of **2-K**, under

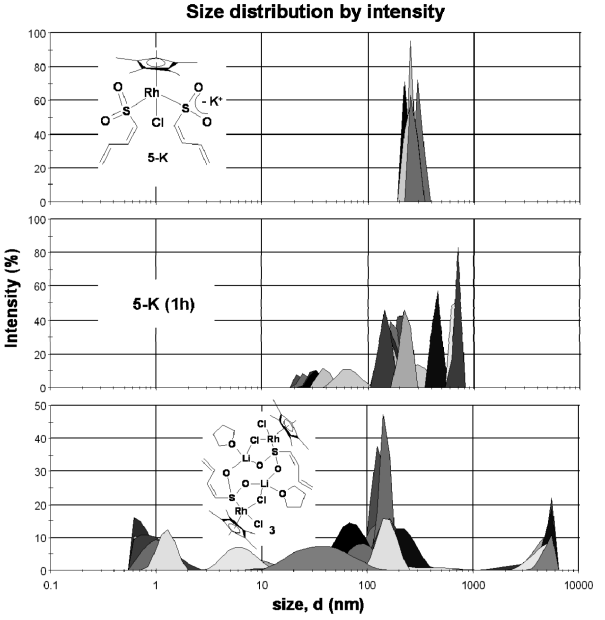

Figure 5. Intensity distribution by DLS of aggregates in compounds (A) **5-K**, (B) **5-K** after 1 h, and (C) **3**.

Scheme 5

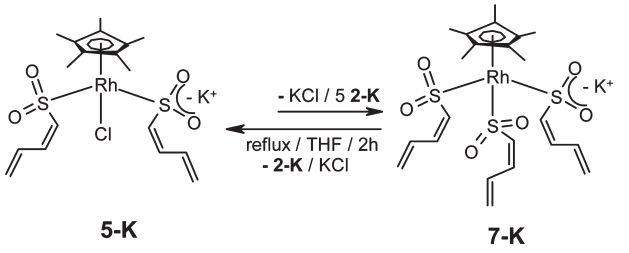

refluxing THF, was carried out in order to verify if more aggregated species could be favored, as occurs in the ruthenium chemistry.[4] The analysis of the mixture by HRMS showed an increase in the formation of **7-K**, along with **5-K**. This result suggests an equilibrium between **5-K** and **7-K** (Scheme 5), in a similar fashion to that observed for ruthenium [Cp*Ru(1,2,5-η-$SO_2CH{=}CHCH{=}CH_2$)(5-η-$S(O_2{}^-K^+)CH{=}CHCH{=}CH_2$)] and [Cp*Ru(5-$\eta$-$S(O_2{}^-K^+)CH{=}CHCH{=}CH_2$)$_2$(5-$\eta$-$SO_2CH{=}CHCH{=}CH_2$)].[4]

In this case, the elimination of KCl from **5-K** along with the addition of **2-K** leads to the formation of **7-K**, which cannot be isolated because it easily loses **2-K**. Comparatively, the lability of **5-K** and **7-K** in solution was lower than that observed in the ruthenium chemistry. Also, it was clear that rhodium chemistry did not favor aggregated species, such as $(\mathbf{5\text{-}K})_n$ or $(\mathbf{7\text{-}K})_n$; instead, the preferred $\mathbf{5\text{-}K(2\text{-}K)_n}$ (n = 1−3) and $\mathbf{7\text{-}K(2\text{-}K)_n}$ (n = 1−2) were observed by mass spectrometry (Figure 6).

In summary, a comparative study between the reactivity of $[Cp^*M(Cl)_2]_2$ (M = Rh, Ir) with ligands **2-Li** and **2-K** has been established, and in general (a) the chemistry of rhodium is shown to be more reactive compared to that of iridium. (b) Rhodium compounds **3** and **5-K** are more labile and unstable compared to those of iridium **3-Ir** and **12**, respectively. (c) The addition reactions give, in the presence of **2-Li**, analogous compounds **3-M** (M = Rh, Ir), while in the presence of **2-K** completely different products are formed. (d) According to neutral compounds **3** and **5-K**, the presence of

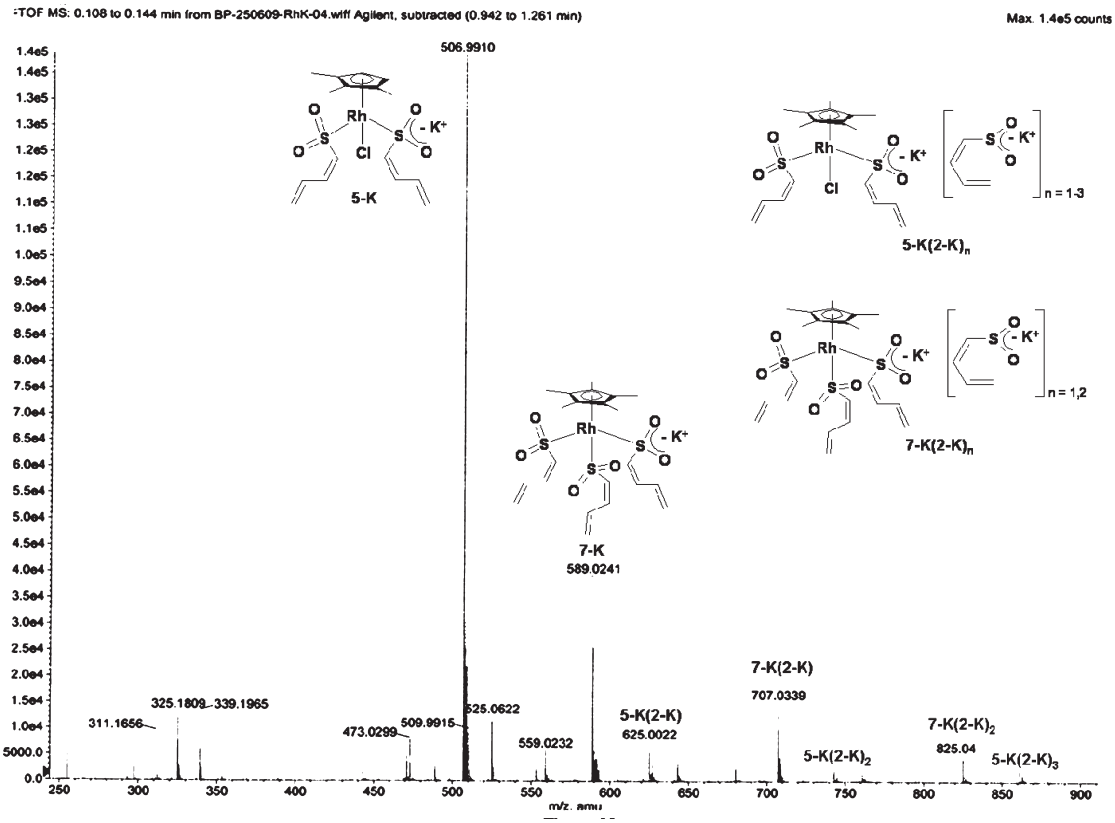

Figure 6. Mass spectrum of the reaction mixture of **5-K** and 5 equiv of **2-K**.

chloro favors exclusively coordination through the sulfur atom, while **12** can easily induce coordination of the sulfur and the terminal double bond of the butadiensulfonyl ligand. (e) Different bonding modes are found for the butadienesulfonyl ligands in the neutral compound **6**. (f) The intrinsic properties of these new butadienesulfinate ligands, which can establish intermolecular interactions, have been corroborated with rhodium complexes, as observed in Figure 6 for **5-K(2-K)**$_n$ (n = 1−3) and **7-K(2-K)**$_n$ (n = 1−2). (g) Complexes **5-K** and **7-K** show the formation of aggregated species, basically through interactions with salt (**2-K**)$_n$ (n = 1−3). Contrastingly, in the ruthenium chemistry, species such as [Cp*Ru(1,2,5-η-$SO_2CH{=}CHCH{=}CH_2$)(5-η-S-($O_2^-M^+$)$CH{=}CHCH{=}CH_2$)]$_n$ (n = 2, 3; M = Li, K) were detected, to which the full ruthenium compounds are aggregated with Li and/or K cations.

Reactivity of 3 and 5-K with PPh_3 and PMe_3. Reactivity of 3 with PPh_3. The reaction of **3** and **5-K** was studied toward PPh_3 and PMe_3 under different reaction conditions. The difference in yields and products formed were due to the influence of the bulkiness and basicity of the corresponding phosphine. Analyses of the mixtures were established by ^1H and $^{31}P\{^1H\}$ NMR (C_6D_6). After stirring **3** with 2.5 equiv of PPh_3, 4 h in toluene at room temperature, compounds Cp*-RhCl(5-η-$SO_2CH{=}CHCH{=}CH_2$)(PPh_3) (**8*S***)[1] and Cp*Rh-$(Cl)_2(PPh_3)$ (**9**)[1,15−17] were detected in 0.1:0.9 ratio, respectively, along with a precipitate of **2-Li**.[1] After 24 h, there was still evidence of **9**, as well as **8-*S***, which partially isomerizes into **8-*W***,[1] in a 0.6:0.2:0.2 ratio (Scheme 6).

An increase in the amount of **8-*S*** is attributed to the metathesis reaction between **9** and **2-Li**, as it also occurs with **2-K**, from which compounds **8-*S*** and **8-*W*** can be efficiently prepared.[1] The same results were observed after 1 h under refluxing THF. From Scheme 6, it is clear that the favored product is the dichloro compound **9**.

The formation *in situ* of the iridium compound **3-Ir**, analogous to **3**, after 1.5 h at room temperature in THF and the presence of 2 equiv of PPh_3, can afford the characteristic elimination of **2-Li**, along with Cp*Ir$(Cl)_2PPh_3$ (**9-Ir**) and Cp*IrCl(5-η-$SO_2CH{=}CHCH{=}CH_2$)(PPh_3) (**8-*S*-Ir**) in a 0.9:0.1 ratio.[6b]

Reactivity of 3 with PMe_3. When compound **3** reacted with 2.5 equiv of PMe_3, elimination of **2-Li** always occurred, as observed in the reactions with PPh_3. A reaction in benzene, at room temperature for 17 h, showed formation of Cp*RhCl-(5-η-$SO_2CH{=}CHCH{=}CH_2$)(PMe_3) (**10-*S***), S=PMe_3, and Cp*Rh$(Cl)_2PMe_3$ (**11**)[15,18−20] in 0.3:0.2:0.5 ratio, respectively.[1] The presence of S=PMe_3 implies that in solution degradation of the butadienesulfonyl ligand has occurred. After 1 h under THF reflux, evidence of **10-*S*** and **11** in a 0.3:0.7 ratio was observed (Scheme 7).

The reaction of the iridium analogue **3-Ir** with 2 equiv of PMe_3, after 1 h at room temperature in THF, showed **2-Li** as well as spectroscopic evidence of **11-Ir**, [Cp*IrCl(5-η-SO_2-$CH{=}CHCH{=}CH_2$)(PMe_3) (**10-*S*-Ir**), and **12** in 0.5:0.3:0.2

(15) Jones, W. D.; Kuykendall, V. L. *Inorg. Chem.* **1991**, *30*, 2615.
(16) Kang, J. W.; Moseley, K.; Maitlis, P. M. *J. Am. Chem. Soc.* **1969**, *91*, 5970.
(17) Singh, S. K.; Trivedi, M.; Chandra, M.; Pandey, S. *J. Organomet. Chem.* **2005**, *690*, 647.
(18) Isobe, K.; Bailey, P. M.; Maitlis, P. M. *J. Chem. Soc., Dalton Trans.* **1981**, 2003.
(19) Paneque, M.; Maitlis, P. M. *J. Chem. Soc., Chem. Commun.* **1989**, 105.
(20) Jones, W. D.; Partridge, M. G.; Perutz, R. N. *J. Chem. Soc., Chem. Commun.* **1991**, 264.

Scheme 6

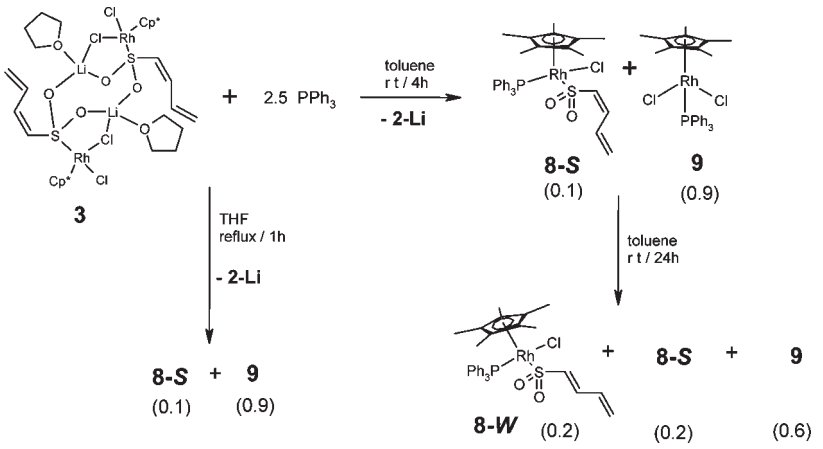

Scheme 7

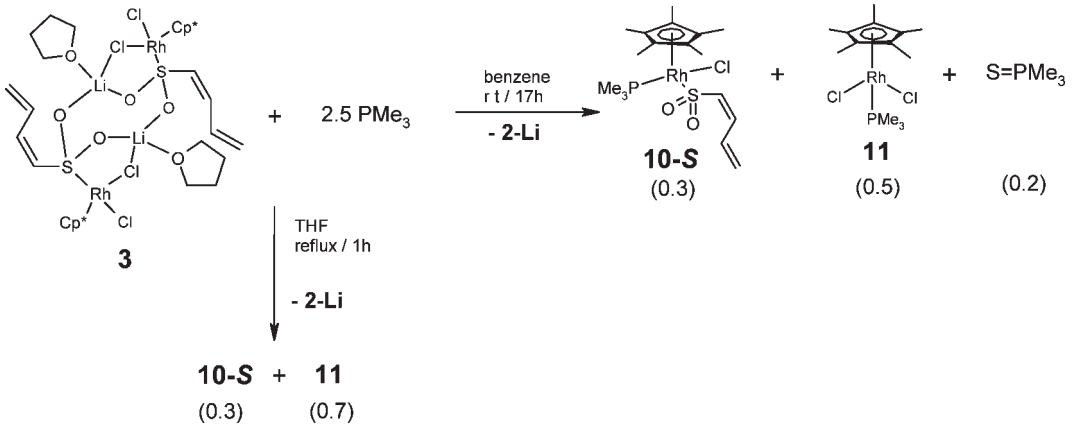

ratio, respectively.[6c] In spite of the lack of selectivity, which is higher for **3** than for **3-Ir**, both compounds favor the formation of the corresponding dichloro compounds [Cp*M-$(Cl)_2PR_3$] [M = Rh, Ir; R = Ph, Me].

Reactivity of 5-K with PPh_3. The chemistry of **5-K** with 2.5 equiv of PPh_3 was explored and summarized in Scheme 8. After 3 h of stirring at room temperature in benzene, compounds **9**, **8-*S***, and **5-K** were observed in 0.2:0.5:0.3 ratio. After 50 h, **5-K** was consumed, **8-*S*** isomerized, and only **8-*W*** and **9** were present, in a 0.7:0.3 ratio. Precipitation of **2-K** and the presence of $O{=}PPh_3$ were always detected by ^1H NMR (D_2O) and $^{31}P\{^1H\}$ NMR (C_6D_6), respectively, along with an unidentified pale orange powder, which did not have any butadienesulfonyl ligand.

The reaction of **5-K** in refluxing THF for 1 h showed the formation of **8-*S***, **8-*W***, **9**, and $S{=}PPh_3$ in a 0.2:0.7:0.1:traces ratio. The reaction of **12** (Scheme 1) with 1.1 equiv of PPh_3 at room temperature in THF during 1 h allowed the isolation of isomers Cp*IrCl(5-η-$SO_2CH{=}CHCH{=}CH_2$)PPh_3 (**8-*S*-Ir** and **8-*W*-Ir**) and Cp*Ir$(Cl)_2PPh_3$ (**9-Ir**)[21] and the recovery of **12** in 25%, 13%, 15%, and 4% yield.[1]

Contrasting with the chemistry of **3**, discussed above, the reactivity of **5-K** with PPh_3 favored the formation of compounds **8-*S*** and **8-*W*** instead of **9**, as well as the isomerization of **8-*S*** to **8-*W***. However, better synthetic procedures through the metathesis reaction of **9** or **11** with **2-K** have been described in the introduction. It has also been established the lack of reactivity of the analogous iridium complex **9-Ir** with **2-K** (1.5 equiv), which only affords **8-*S*-Ir** in 6% yield, and the isomerization from *S*- to *W*-derivatives does not occur.[1]

The corresponding chemistry of **5-K** with PMe_3 was even less selective and gave a complex mixture. The reaction of iridium **11-Ir** with **2-K** affords **10-*S*-Ir** in 62% yield, and only traces of **10-*W*-Ir** were observed, without further evidence of isomerization of **10-*S*-Ir** to **10-*W*-Ir**.[1]

The isomerization process of the rhodium derivatives **8-*S*** and **10-*S*** was studied by ^1H NMR. Compound **10-*S*** showed slower transformation than the corresponding **8-*S***. After 5.5 h at 55 °C the isomerization of **10-*S*** to **10-*W*** was complete, while compound **8-*S*** fully isomerized to **8-*W*** after 1 h at 60 °C. The isomerization of **10-*S*** and **8-*S*** also occurs after 3 h of reflux in toluene or 1.5 h in THF, respectively. In order to explain these observations, the crystalline structures of **10-*S***, **10-*S*-Ir**,[1] and **8-*S*-Ir**[6d] were analyzed (*vide infra*). The isomerization requires the rotation of the C3−C4 bond, which should be long enough to diminish the double-bond character and induce an easier rotation. The rhodium complex **10-*S***, compared to the iridium isomers **8-*S*-Ir** and **10-*S*-Ir**, showed the faster isomerization, along with the longest C3−C4 bond length [1.395(14) Å] compared to those of **8-*S*-Ir** [1.337(17) Å] and **10-*S*-Ir** [1.343(16) Å]. A tentative isomerization process is described in Scheme 9, which implies the formation of a cationic sulfene in the transition state.

(21) Booth, B. L.; Haszeldine, R. N.; Hill, M. *J. Organomet. Chem.* **1969**, *16*, 491.

Scheme 8

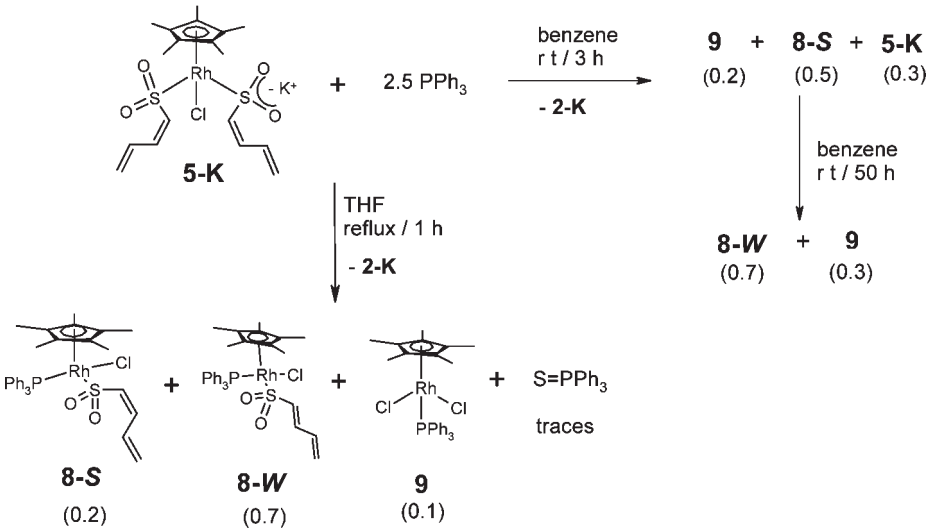

Scheme 9

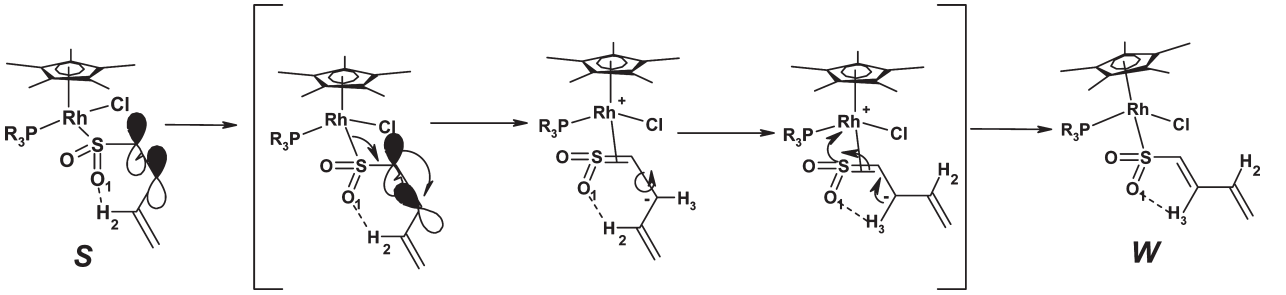

This statement is mainly supported by the existence of thioaldehyde rhodium compounds.[22]

It is assumed that the *W*-isomer is more stable because the pseudo-ring in the *S*-conformer has six atoms [H2−O1−S−C4−C3−C2], while in the *W*-conformer only five atoms [H3−O1−S−C4−C3] form the pseudo-ring. Along with this, it is well known that in substituted dienes the *E*-conformer is more stable than the corresponding *Z* due to steric effects. In the rhodium and iridium molecules, the *S*- and *W*-isomers are the *Z*- and *E*-conformers, respectively. Scheme 9 shows that, in order to get the *W*-conformer, the isomer *S* promotes the torsion of the C3−C4 sp^2 bond. This process occurs by twisting the C3−C4 bond, until a sp^3 bond is formed, hence generating a cationic sulfene with a negative charge over C3. This is the transition state, which is formed with the promotion of one electron from the C4 π orbital to a sp^3 orbital of C3. After the rotation of the C3−C4 bond, migration of the negative charge from C3 to C4 occurs, along with the formation of the Rh−S σ-bond by the promotion of the π-density of the double bond S=C4, thus giving the thermodynamic *W*-isomer. It is proposed that the transition state is more efficiently stabilized if there is a low electron density in the metal. This statement could explains why **8-*S*** isomerizes faster than **10-*S***, in which the less basic and better acceptor properties of the PPh_3 may decrease the energy of the activated state, while the more basic and less efficient acceptor PMe_3 would increase in energy.

The molecular structure of compound **10-*S*** (Figure 7) is isostructural with **10-*S*-Ir**,[1] where the rhodium atom coordinates PMe_3, Cl, Cp*, and the η^1-butadienesulfonyl ligand. Crystal data are given in Table 1, and selected bond lengths and angles are in Table 2. The dihedral angle C1−C4 of 178.57(1.13)° confirms the *S*-conformation, and due to the formation of hydrogen bonds H2−O1 [2.367(7) Å] and H4−Cl [2.911(3) Å], two pseudo-rings of six and five members are respectively formed among H2−O1−S−C4−C3−C2 and H4−Cl−Rh−S−C4.

The crystal structure of the rhodium compound **9** was not found in the Cambridge database, even though it is a well-known and useful precursor. The ORTEP diagram is shown in Figure 8, and the crystal data are given in Table 1. The molecule is isostructural with iridium **9-Ir** already described.[1,23] The longest Rh1−P1 bond length of **9** [2.3408(18) Å] compared with the iridium half-sandwich **9-Ir** [2.3182(14) Å][1] suggests the lability of the PPh_3 in the rhodium compound.

In summary, under several conditions, addition reactions of compounds **3** and **5-K** showed no selectivity with PPh_3 or PMe_3. The more basic phosphine gives the highest reactivity, and in all cases, the dichloro complexes **9** and **11** are formed.

(22) Bleeke, J. R.; Shokeen, M.; Wise, E. S.; Rath, N. P. *Organometallics* **2006**, *25*, 2486.

(23) Le Bras, J.; Amouri, H.; Vaisserman, J. *J. Organomet. Chem.* **1997**, *548*, 305.

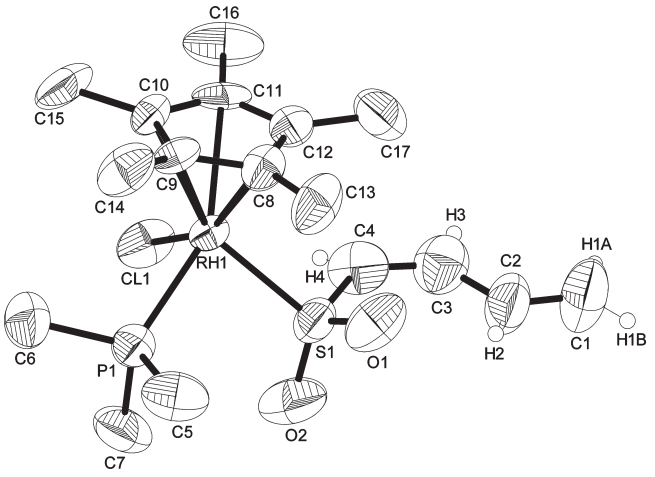

Figure 7. Crystal structure of compound [Cp*RhCl(5-η-SO_2-CH=CHCH=CH_2)(PMe_3)] (**10-*S***).

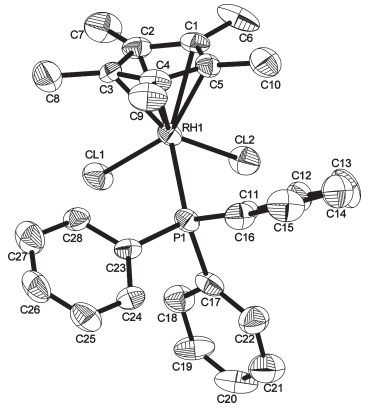

Figure 8. Crystal structure of compound [Cp*Rh$(Cl)_2$(PPh_3)] (**9**).

This reaction is favored when **3** was used as precursor, instead of **5-K**. Comparison between the rhodium and iridium chemistry showed that the rhodium derivatives are more reactive and less selective. Comparison between the rhodium and ruthenium chemistry showed that different bonding modes could be generated depending on the electronic properties of each metal. The aggregated species are favored in the ruthenium chemistry, while intermolecular interactions were observed only for rhodium. The presence of the SO_2 in the heterodienyl ligand modifies significantly the structural and electronic properties of the corresponding metallic derivatives compared to those obtained from $(Cp^*RuCl)_4$ and $(Cp^*MCl_2)_2$ (M = Rh, Ir) with oxo-, aza-, and thiapentadienyl ligands.

Experimental Section

General Procedures. Standard inert-atmosphere techniques were used for all syntheses and sample manipulations. The corresponding lithium and potassium butadienesulfinate salts **2-M** (M = Li, K) were freshly prepared and, along with **3** and $AgBF_4$, were weighed in a glovebox. Solvents were dried by standard methods (diethyl ether and THF with Na/benzophenone, toluene and benzene with metallic Na, pentane with CaH_2, and acetone with K_2CO_3) and distilled under nitrogen prior to use. Compounds $[Cp^*RhCl_2]_2$[24] and potassium or lithium butadienesulfinate (**2-M**) (M = Li, K) were prepared according to literature procedures.[1,2] Compounds **8*S***,[1] **8*W***,[1] **9**,[15,16] **10-*S***,[1] and **11**[1,15,18] have been previously reported. All other chemicals were used as purchased from Sigma-Aldrich, Fluka, Strem Chemicals, Merck, J. T. Baker, Isotec, and Cambridge Isotopes. Elemental analyses were performed at Cinvestav, using a Thermo-Finnigan Flash 112 for C, H, N, and S. The melting points were determined using a Gallenkamp melting point apparatus and are uncorrected. IR spectra were recorded on a Perkin-Elmer 6FPC-FT spectrophotometer using KBr with NaCl plates. ^{1}H, ^{13}C, and ^{7}Li NMR spectra were recorded on Jeol GSX-270, Eclipse+400 MHz, or Bruker 300 MHz spectrometers in dry, deoxygenated, deuterated solvents. ^{1}H and ^{13}C NMR chemical shifts are reported relative to the residual protium resonance in the solvent,[25] ^{7}Li relative to LiCl, and ^{31}P relative to H_3PO_4.

Mass Spectrometry. ESI mass spectra were recorded in positive- and negative-ion modes using an Agilent G1969A electrospray-ionization time-of-flight spectrometer with an average of 11 scans. The analyte solutions (approximately 0.3 mM in acetone) were delivered to the mass spectrometer source using a G1312A_1 bin pump. Assignment of major ions was aided by a comparison of the experimental and calculated isotope distribution patterns. A fragmentor voltage of 215 V and a flow rate of 0.4 mL/min using MeCN as mobile phase were used for all the experiment acquisitions. Reactions of **1** with **2Li** (1:10) and with **2-K** (1:10) and of **5-K** with **2-K** (1:5) were carried out under reflux of THF for 2 h in the case of **1** and 3 h for **5-K**. An analyte of the filtered and evaporated mother liquors from each reaction was taken, and their spectra were acquired.

Dynamic Laser Light Scattering (DLS) Instrumentation and Measurements.[26] The samples of **3** and **5-K** were prepared in THF at highly diluted concentrations, then filtered through a Millipore 0.5 μm LCR filter for dust removal and poured in a quartz cell. A commercial DLS spectrometer (Malvern Zetasizer Nano 90) equipped with a fast correlator card (minimum sample time is 12.5 ns) and temperature control from 2 to 90 °C was used for measurements. A He−Ne laser operated at 633 nm and 4.0 mW was used as the light source using a multiple narrow method. The primary beam was vertically polarized. Scattered intensity was taken at 90° to the incident beam. For the calculation of the hydrodynamic radius (R_h) in THF, values of 0.4549 and 1.409 were used for the viscosity (η) and the refractive index (RI), respectively.

Crystal Structure Determination. Crystals suitable for X-ray diffraction of compound **3** were obtained from indirect Et_2O diffusion to a concentrated THF solution of **3** at −15 °C. The red crystal was mounted in a capillary under an ethereal atmosphere. Yellow needles of compound **10-*S*** were obtained when Et_2O was slow added to a concentrated solution of **10-*S*** in cold acetone. A yellow needle was mounted on a capillary. Crystals of **9** were grown from slow evaporation of a $CHCl_3$ concentrated solution, and in the unit cell a molecule of chloroform is present. The X-ray diffraction measurements were made at 173(2) K on an Enraf Nonius-Kappa CCD diffractometer with $\mu(Mo/K\alpha)_{calc}$ 0.71073 mm^{-1}.

The structures were solved by direct methods (**9** and **10-*S***) and by the heavy-atom method (**3**) using SHELX-97[27] included in WinGX[28] and refined by a full-matrix least-squares method based on F^2. Absorption correction was performed with Multi-Scan. All non-hydrogen atoms were refined with

(24) White, C.; Yates, A.; Maitlis, P. M. *Inorg. Synth.* **1992**, *29*, 228.

(25) Gottlieb, H. E.; Kotlyar, V.; Nudelman, A. *J. Org. Chem.* **1977**, *62*, 7512.

(26) (a) Low, P. M. N.; Yong, Y. L.; Yan, Y. K.; Hor, T. S. A.; Lam, S.-L.; Chan, K. K.; Wu, C.; Au-Yeung, C. F. S.; Wen, Y.-S.; Liu, L.-K. *Organometallics* **1996**, *15*, 1369. (b) http://www.malvern.com.

(27) Sheldrick, G. M. *SHELXL*, Program for Crystal Structure Refinement; University of Göttingen: Göttingen, Germany, 1998.

(28) Farrugia, L. J. *J. Appl. Crystallogr.* **1999**, *32*, 837.

anisotropic thermal displacement coefficients unless specified otherwise.

Electrochemical Experiments. Tetrabutylammonium tetrafluoroborate 99% (n-Bu_4NBF_4) was used as the supporting electrolyte, and freshly distilled THF was used as solvent. All solutions were purged with high-purity argon before each run and maintained over inert atmosphere during the experiment. The electrochemical apparatus consisted of a DEA-332 potentiostat (Radiometer Copenhagen) with positive feedback resistance compensation. A conventional three-electrode cell was used to carry out the voltammetric experiments. A glassy carbon disk of 3 mm diameter was used as working electrode (Sigradur G from HTW, Germany). Prior to its use, it was carefully polished with 0.3 μm alumina powder (Büehler), rinsed with distilled water, and sonicated in ethanol. The counter electrode was a platinum mesh. The reference electrode was an aqueous saturated calomel electrode, SCE. A salt bridge, which contained 0.2 M of the corresponding supporting electrolyte in THF, connected the cell with the reference electrode. All electrochemical experiments were performed at 25 °C.

Synthesis of [Cp*Rh(Cl)$_2$(SO$_2$CH=CRCH=CHR)(Li)(THF)]$_2$ (3). Compound **1** (150 mg, 0.243 mmol) and salt **2-Li** (91 mg, 0.733 mmol) were placed in a Schlenk with a magnetic stirrer. Solids were purged under vacuum 5 min, and after that, the system was saturated with N_2 atmosphere. The system was cooled at −110 °C (liq N_2/EtOH), THF (15 mL) was added, and the mixture was stirred until it reached room temperature; then stirring continued for 2 h more. The solution was filtered and the volume was reduced until 5 mL, diethyl ether was added (15 mL), and the mixture was left at −15 °C. Red crystals precipitated along with a bright orange powder in 82% yield (100 mg, 0.100 mmol). The solution was filtered, and crystals were separated manually from the orange powder. The solid compound was highly labile in the presence of traces of water, which turned sticky, and finally into a dark red powder. Compound **3** was always manipulated in a drybox, and the melting point was not obtained. ^{1}H NMR (C_6D_6): δ 5.39 (d, J = 8.9 Hz, 1H, H1′$_{gem}$), 5.20 (d, J = 17.0 Hz, 1H, H1$_{gem}$), 8.19 (m, 1H, H2), 5.98 (t, J = 11.2 Hz, 1H, H3), 6.79 (d, J = 11.0 Hz, 1H, H4), 1.43 (s, 15H, Cp*), 3.64 (m, 4H, CH_2-O, THF), 1.46 (m, 4H, CH_2-CH$_2$-O, THF). ^{13}C{^{1}H} NMR (TDF): δ 123.8 (C1), 133.0 (C2), 132.7 (C3), 136.5 (C4), 8.8 (Cp*), 98.1(d, J = 7.0 Hz, Cp*), 67.8 (*C*H$_2$-O, THF), 25.5 (*C*H$_2$-CH$_2$-O,THF). ^{7}Li NMR (C_6D_6): δ 5.26. IR (THF): 1789 (m), 1763 (m), 1700 (m), 1639 (w), 1457 (w), 1376 (w), 1346 (w), 1228 (w), 1204 (s), 1148 (vs), 1118 (vs), 1071(vs, br), 1043 (vs, br), 1027 (sh), 994 (vs, br), 951 (sh), 912 (m), 892 (m), 884 (m), 858 (vs, br), 674 (w, br), 411 (m) cm^{-1}.

Synthesis of [Cp*RhCl(5-η-SO$_2$CH=CHCH=CH$_2$)(5-η-S(O$_2^-$K$^+$)CH=CHCH=CH$_2$)] (5-K). The reaction was carried out via a similar procedure to the one described for **3**, but with **1** (150 mg, 0.243 mmol) and **2-K** (190 mg, 1.22 mmol). After concentration of the filtered mother liquor and addition of pentane (70 mL), the mixture was left at −15 °C. Filtration afforded an orange powder in 90% yield (154.5 mg, 0.282 mmol). **5-K** decomposed at 140 °C. ^{1}H NMR (acetone-d_6): δ 5.24 (d, J = 10.1 Hz, 1H, H1′$_{gem}$), 5.31 (d, J = 17.1 Hz, 1H, H1$_{gem}$), 7.85 (m, 1H, H2), 6.02 (t, J = 11.1 Hz, 1H, H3), 6.55 (d, J = 11.3 Hz, 1H, H4), 1.57 (s, 15H, Cp*). ^{13}C{^{1}H} NMR (acetone-d_6): δ 121.2 (C1), 133.1 (C2), 128.8 (C3), 139.9 (C4), 8.2 (Cp*), 102.2 (d, J = 5.4 Hz, Cp*). IR (KBr): 3081 (w), 3042 (w), 2999 (m), 2910 (m), 1626 (m, br), 1571 (s), 1499 (m), 1477 (sh), 1453 (m, br), 1413 (sh), 1377 (m), 1357 (w), 1329 (w), 1304 (w, br), 1279 (sh), 1231 (m), 1175 (vs, br), 1111 (s), 1050 (vs, br), 1027 (sh), 951 (m), 918 (s, br) 787 (s), 713 (m), 664 (vs, br), 573 (w, br), 539 (s), 471 (s), 411 (w) cm^{-1}. EI: m/z 450 (100), 391 (1), 292 (6), 238 (25), 64 (58), 54 (14), 48 (26). ESI-TOF-MS: (negative) 506.9934 uma, error −1.8392 ppm. Anal. Calcd for $C_{18}H_{25}ClKO_4S_2Rh$ (546.99): C 39.97, H 4.63, S 11.50. Found: C 39.52, H 4.62, S 11.73.

Synthesis of [Cp*Rh(1,2,5-η-SO$_2$CH=CHCH=CH$_2$)(5-η-SO$_2$CH=CHCH=CH$_2$)] (6). The reaction was carried out via a similar procedure to the one described for **3**, but with **5-K** (250 mg, 0.458 mmol) and $AgBF_4$ (90 mg, 0.462 mmol). The system was cooled to −110 °C (liq N_2/EtOH), and THF (35 mL) was added. Immediately after that, the cold bath was removed and the system was stirred for 45 min. KBF_4 and AgCl precipitated. After five filtrations, evaporation, and recrystallization [THF/pentane (1:7), −15 °C] of the liquid phase, a bright yellow powder was obtained in 67% yield (145.0 mg, 0.307 mmol). **6** decomposed at 144−148 °C. ^{1}H NMR (acetone-d_6): (ligand 5-η): δ 4.20 (d, J = 9.2 Hz, 1H, H1′$_{gem}$), 3.89 (d, J = 13.1 Hz, 1H, H1$_{gem}$), 5.86 (t, J = 11.8 Hz, 1H, H2), 6.27 (d, J = 7.0 Hz, 1H, H3), 6.10 (d, J = 6.7 Hz, 1H, H4); (ligand 1,2,5-η): 5.34 (d, J = 10.0 Hz, 1H, H1′$_{gem}$), 5.42 (dd, J = 17.1, 0.9 Hz, 1H, H1$_{gem}$), 7.71 (dt, J = 17.1, 10.8 Hz, 1H, H2), 6.22 (d, J = 11.2 Hz, 1H, H3), 6.94 (d, J = 11.0 Hz, 1H, H4), 1.80 (s, 15H, Cp*). ^{13}C{^{1}H} NMR (acetone-d_6): (ligand 5-η) δ 74.7 (d, J = 8.5 Hz, C1), 102.6 (d, J = 8.5 Hz, C2), 128.0 (d, J = 2.3 Hz, C3), 153.1 (d, J = 6.9 Hz, C4); (ligand 1,2,5-η): 123.3 (C1), 132.4 (C2), 132.3 (C3), 143.7 (C4), 7.8 (Cp*), 108.6 (d, J = 4.6 Hz, Cp*). IR (KBr): 3053 (w), 3008 (w), 2972 (w), 2919 (w), 1704 (m), 1624 (m), 1569 (m), 1477 (m), 1424 (m), 1380 (m), 1297 (m), 1178 (vs, br), 1116 (sh), 1048 (vs, br), 810 (m), 772 (w), 739 (m), 663 (s), 627 (sh), 535 (s), 474 (m), 438 (m) cm^{-1}. ESI-TOF-MS: (positive) 473.0329 uma, error 1.4637 ppm; (negative) 471.0178 uma, error 0.3084 ppm. Anal. Calcd for $C_{18}H_{25}O_4S_2Rh$ (472.41): C 45.76, H 5.34. Found: C 45.61, H 5.32.

Reactivity Studies of Compound 1 with 2-Li and 2-K. 1 (20.0 mg, 0.032 mmol) and **2-Li** (40.0 mg, 0.320 mmol) or **1** (50.0 mg, 0.081 mmol) and **2-K** (125.0 mg, 0.800 mmol) were placed into a Schlenk flask equipped with a stirring bar. THF was added (10 mL), and the mixture was stirred under reflux for 2 h. The solution was cooled and filtered, and the solvent was removed under vacuum. The sample was analyzed by HRMS (positive and negative ESI-TOF-MS in acetone, using a fragmentor voltage of 150 V and 100% of NCMe as mobile phase). The species **5-Li** and **(5-Li)$_2$** were observed in 2:1 ratio, while the potassium species **5-K**, **(5-K)$_2$**, and **7-K** were detected in 9.0:0.5:1.0 ratio, respectively (see Supporting Information).

Reactivity Studies of Compound 5-K with 2-K. A procedure similar to the one used for the reaction previously described, but with **5-K** (50.0 mg, 0.092 mmol) and **2-K** (72.0 mg, 0.461 mmol), was carried out. The mixture was refluxed in THF (10 mL) for 3 h and filtered and the solvent evaporated until dryness. The powder obtained was studied through ^{1}H NMR ($CDCl_3$, Supporting Information) and ESI-TOF-MS in negative mode, Figure 6.

General Method of Preparation of Complexes 8-*S*, 8-W, 9, 10-*S*, and 11 through Reactivity of 3 and 5-K with PPh$_3$ and PMe$_3$. A mixture of **3** (50.0 mg, 0.050 mmol) and 2.5 equiv of PPh_3 (33.0 mg, 0.126 mmol) was stirred in toluene (10 mL) at room temperature for 4 and 24 h or under reflux of THF (15 mL) during 1 h. A similar reaction was carried out with **5-K** (50.0 mg, 0.091 mmol) and 2.5 equiv of PPh_3 (60.0 mg, 0.229 mmol) in benzene (10 mL) at room temperature for 3 and 50 h, or under reflux of THF (15 mL) during 1 h.

A mixture of **3** (50.0 mg, 0.050 mmol) and 2.5 equiv of PMe_3 (9.5 mg, 0.125 mmol) was stirred in benzene (10 mL) at room temperature for 17 or 1 h under reflux of THF (15 mL).

Acknowledgment. This work was financially supported by the National Council of Science and Technology (Conacyt) (46556-Q). B.P.M. is grateful for a scholarship from Conacyt. We thank Dr. Ilia A. Guzei for advising in the crystal structure determination, M. S. S. Buendía Aceves and Dr. M. E. Navarro-Clemente from ESIQIE/IPN for use and assistance with the DLS equipment, and

M. Cervantes-Vasquez, M. A. Leyva, and G. Cuellar for technical support in experimental work, the X-ray diffraction, and ESI-TOF-MS, respectively.

Supporting Information Available: Crystallographic and refinement details for compounds **3** (CCDC-758496), **9** (CCDC-758497), and **10-*S*** (CCDC-758498); additional information on ^{1}H NMR spectra of **5-K**, **6**, and a mixture of **5-K** and **7-K** is included, as well as mass spectra of the reaction of **1** with **2-Li** and **2-K**. This material is available free of charge via the Internet at http://pubs.acs.org. Supplementary crystallographic data can be obtained, free of charge, from The Cambridge Crystallographic Data Centre via www.ccdc.cam.ac.uk/data_request/cif.